European Journal of Plant Pathology **102:** 51–60, 1996.

Spread of faba bean rust over a discontinuous field

I. Sache[1,2] and J. C. Zadoks[1]

[1]*Department of Phytopathology, Wageningen Agricultural University, P.O. Box 8025, 6700 EE Wageningen, The Netherlands;* [2]*Permanent address: Laboratoire de Pathologie Végétale, INRA, 78850 Thiverval-Grignon, France (Fax: 1 30 81 53 06)*

Accepted 19 May 1995

Key words: biological invasion, focus expansion, spatio-temporal processes, spore dispersal, *Uromyces viciae-fabae, Vicia faba*

Abstract

Spatio-temporal progress of an epidemic of faba bean rust was monitored over a discontinuous field. Trap plots were sown at increasing distances from a source plot, in the centre of which plants were inoculated. Disease spread in the source plot followed a focal pattern, with a radial velocity of expansion slightly lower than 0.1 m per day. At the end of the experiment, all trap plots had been infected, and two of the most distant ones showed unexpected high disease severity. Using a three-dimension model of disease progress, we showed that the epidemics on the scales of the source plot and of the trap plots could not be combined into a single epidemic on the whole-field scale. The epidemics had equivalent infection rates on both scales, but changing the scale dramatically affected their distance parameter. The epidemic in the source plot could have been caused by a short-distance, high-frequency, deterministic mechanism of spore dispersal, whereas infection of the trap plots could have been caused by a long-distance, low-frequency stochastic mechanism of spore dispersal. Although our results agreed with the predictions of a simulation model postulating these two mechanisms, alternative hypotheses which could also explain the observed disease pattern remained to be tested.

Introduction

Empirical evidence is available for various scales of spatio-temporal development of plant disease epidemics, but the relationships between epidemics occurring on different scales have not been established quantitatively. Most theoretical work dealt with focus expansion within a single field [e.g. Zadoks and Kampmeijer, 1977; Minogue and Fry, 1983a; Van den Bosch *et al.*, 1988b], and the proposed models were validated by field experiments [Minogue and Fry, 1983b; Van den Bosch *et al.*, 1988a, 1990].

Considering spore escape from a disease focus, Gäumann [1946] opposed the large quantity of spores reaching 'the receiver in short-range infection' to the 'sparse and long-range infections [which] are important because they extend the infection chain by leaps and bounds'. Vanderplank [1967] developed the idea in terms of gradients, the short-range infection being associated with a steep gradient and focus enlargement, and the long-range infections being associated with a shallow gradient and initiation of new foci. Based on a physical approach of these concepts, a mathematical model postulated two mechanisms leading to short-distance, high-frequency, and long-distance, low-frequency dispersal. The two postulated mechanisms differed by their range of spore dispersal, related to the spore diffusion coefficient and deposition rate [Zawolek and Zadoks, 1992; Zawolek, 1993]. Association of both mechanisms might explain disease spread over discontinuous cultivated areas, such as a mosaic of fields scattered over a large geographic area, and continental expansion of epidemics.

Assuming that equivalent mechanisms would occur on a smaller, attainable to field experiment, spatial scale, we report here the results of a pilot, non-replicated field study designed to monitor disease spread from an inoculated focus over a discontinuous

field. The pathosystem used, faba bean (*Vicia faba*) – rust (*Uromyces viciae-fabae*), has adequate features in Wageningen for that purpose, i.e., temperature and dew duration favourable to infection during the host growing season, focal spread of epidemics, no natural sources of inoculum, and no risk of economic losses due to accidental spread of the disease to cultivated fields. The objective of the study was to monitor the spread of disease across the inoculated source plot (primary focus) and to distant, non-inoculated trap plots (secondary foci). Using simple temporal [Vanderplank, 1963], spatial [Gregory, 1968; Kiyosawa and Shiyomi, 1972] and spatio-temporal [Jeger, 1983] models, disease spread was characterized by rate and distance parameters on the scales of the source plot, the trap plots, and the whole field (source and trap plots). The relationships between the disease spread on these scales and the two postulated mechanisms of spore dispersal were then discussed.

Materials and methods

Field layout. In a maize (*Zea mays*) field (75×50 m) located in Wageningen, plots of faba bean cv 'Alfred' (Cebeco Zaden BV, Rotterdam), highly susceptible to rust, were sown by hand on 16 March 1993. The 'source plot' consisted of 13×13 units, planted at a centre-to-centre distance of 0.3 m. Each 'unit' consisted of 3 seeds producing 2–7 stems. Thirty-three 'trap plots' were established following a regular pattern (Fig. 1). Five rows of 3, 5, 7, 6, and 9 trap plots were established downwind from the source plot at 10 m, 20 m, 30 m, 35 m, and 40 m, respectively. Three trap plots were established 10 m upwind from the source plot. Rows ran NW to SE, perpendicular to the prevailing SW wind. Distance between plots within rows was 10 m. Each trap plot consisted of 3×3 units, planted at a centre-to-centre distance of 0.3 m. All plots were sprayed with cyfluthrin (15 g a. i..ha^{-1}) to control pea weevil (*Sitona lineatus*) 51 days after planting (DAP) and weeded by hand 69 DAP.

Rust inoculation. The central unit of the source plot was fenced off with plastic sheets and inoculated 69 DAP late in the afternoon. A suspension of urediniospores (*c.* 10^6 urediniospores.ml^{-1}) in mineral oil (Soltrol 170, Phillips Chemical Co., Bartlesville, USA) was sprayed onto the leaves until run-off. The inoculated unit was covered with a plastic tent during the following night to promote urediniospore germination, penetration, and infection.

Disease assessment. Disease severity was assessed in regular rounds twice a week up to 38 days after inoculation, due to extremely rapid spread of the epidemic. Later on and up to 59 days after inoculation, disease severity was assessed only once a week to limit canopy disturbance and spore dispersal by the observer. In every round the observer worked progressively across the plots with least infection to those more heavily rusted, and scored the source plot at the end of the round. Sporulating lesions were counted on each leaf and forty sporulating lesions per leaf were considered to equal 1% severity. Severity levels higher than 5% were scored using an unpublished pictorial key designed by M. W. Hoogkamer (Department of Phytopathology, Wageningen Agricultural University) since lesion counting was no more possible. Mean severity was evaluated for each unit by averaging severity values recorded for all leaves of the unit.

Epidemic in the source plot. All calculation methods used in this section assume isodiametric focus expansion. Distances (d, 27 values, range 0–2.55 m) are centre-to-centre distances between the inoculated and the target units. Using disease severity (x) averaged per distance, the apparent infection rate (r_s) was estimated at each distance by linear regression [Vanderplank, 1963]:

$$\text{logit}(x) = \text{intercept} + r_s.t \qquad (1)$$

Using severity averaged per distance, the slope (b) of the disease gradient was estimated at different dates (from 21 to 59 days after inoculation) after linearization of the exponential model [Kiyosawa and Shiyomi, 1972]:

$$\ln(x) = \text{intercept} - b_e.d \qquad (2)$$

and after linearization of the power law model [Gregory, 1968]:

$$\ln(x) = \text{intercept} - b_p.\ln(d) \qquad (3)$$

The radial expansion velocity (c) was calculated for different isopaths (annuli with severity equal to a given level at a given date [Berger and Luke, 1979]) at levels ranging from 1% to 50% severity. The area within the isopath (A) was calculated from isopath scale maps, assuming a constant area of 0.09 m^2 per unit. Assuming a constant radial expansion velocity during focus expansion, c was estimated by linear regression [Van den Bosch *et al.*, 1992]:

$$(A/\sqrt{\pi}) = \text{intercept} + c.t \qquad (4)$$

Epidemics in the trap plots. Each trap plot was represented by severity averaged over its nine units. Apparent infection rate (r_t) was estimated for each plot as described above. Mean severity per trap plot at different dates was plotted against the distance between the centre of the source and the centre of each trap plot (17 values, range 10–57 m) to determine the disease gradient of the epidemic over all trap plots. The slope (B) of the disease gradient was estimated as described above. Estimations of B were made with and without data from the two trap plots #20 and #22, which showed unexpected high severity (Fig. 1).

Relationships between epidemics in source and trap plots. Characteristics of the epidemics were used to select *a priori* three-dimensional models [Jeger, 1983]. Among the eight models available, only models for 'classical polycyclic diseases' and 'the early stages of a polycyclic epidemic initiated by artificial inoculation at a plot centre', further referred as 'classical' and 'focal', respectively, were consistent with the observed epidemics. The linearized models were fitted to the mean severity by multiple linear regression:

$$\ln(x) = \text{intercept} + b_c.d + r_c.t \quad (\text{'classical model'}) \qquad (5)$$

$$\ln(x) = \text{intercept} + b_f.\ln(d) + r_f.t \quad (\text{'focal model'}) \qquad (6)$$

Models were fitted to data from (*i*) the source plot (*ii*) the trap plots, including #20 and #22, (*iii*) the trap plots, excluding #20 and #22, and all plots, (*iv*) including #20 and #22 or (*v*) excluding #20 and #22. From the classical model (equation [5]), the relaxation distance α, i.e., the distance from the centre or the source plot at which the predicted disease severity decreases by $1/e$ [Zadoks and Schein, 1979], was calculated:

$$\alpha = 1/b_c \qquad (7)$$

α was used as a distance parameter to compare the epidemics occurring on the different scales of the study.

Results

Epidemic in the source plot. Sporulation began on the inoculated unit on day 10 after inoculation and continued up to the death of the plants on day 59. Other units of the source plot did not show rust lesions before day 20. All units were infected on day 31. There was no obvious directional effect in focus enlargement. The assumption of isodiametric expansion of focus, thus, was confirmed and the data were averaged over directions for each distance from the centre.

Disease progress curves were plotted for various distances from the centre (Fig. 2A). A logistic pattern was found for most distances up to 1.2 m. For longer distances, host tissue was not saturated by disease on day 59, and the pattern of disease progress was exponential. Local apparent infection rates (r_s) were in the range 0.21 (at $d = 2.55$ m)–0.29 (at $d = 0.67$ m) d^{-1}.

Disease gradient became steeper with time up to day 35, and flattened from day 44 onwards (Fig. 2B). The primary disease gradient was established during the third latent period after inoculation [Savary, 1987], here on day 35. The best fit was obtained with the power law model during the build-up of the primary disease gradient and later with the exponential model. The dimensionless slope of the primary disease gradient calculated with the power law model was $b = 2.11$.

The spatio-temporal spread followed a focal pattern. The three usual stages of focus expansion, *i.e.* focus build-up without focus enlargement (days 10 to 23), focus expansion at constant radial velocity (days 23 to 52), and breakdown of focus expansion due to plot saturation (days 52 to 59), are shown on Fig. 3. The radial expansion velocity c was estimated using equation (4) applied to the straight lines drawn in the expansion phase. The isopath level had little effect on c, which reached 0.08 $m.d^{-1}$ for isopath levels lower than 10%, 0.07 $m.d^{-1}$ for 15–25% isopath levels, and 0.09 $m.d^{-1}$ for higher isopath levels.

Epidemics in the trap plots. Sporulating lesions were observed on day 28 in one unit in each of four plots (#1, #2, #6, #20). All units of all plots were infected on day 59. The trap plots #20 and #22, located at 38 m and 57 m from the centre, respectively, exhibited a much higher disease severity than their neighbouring plots (Fig. 1). When all plots were considered, there was a significant correlation between the time of first rust observation and the distance from the source plot ($r = 0.48$, $P = 0.005$). Final disease severity (day 59) was not correlated with the distance from the source plot ($P = 0.57$). When the trap plots #20 and #22 were excluded, the correlation between the time of first rust observation and the distance from the source plot increased ($r = 0.60$, $P = 0.003$). Final disease severity

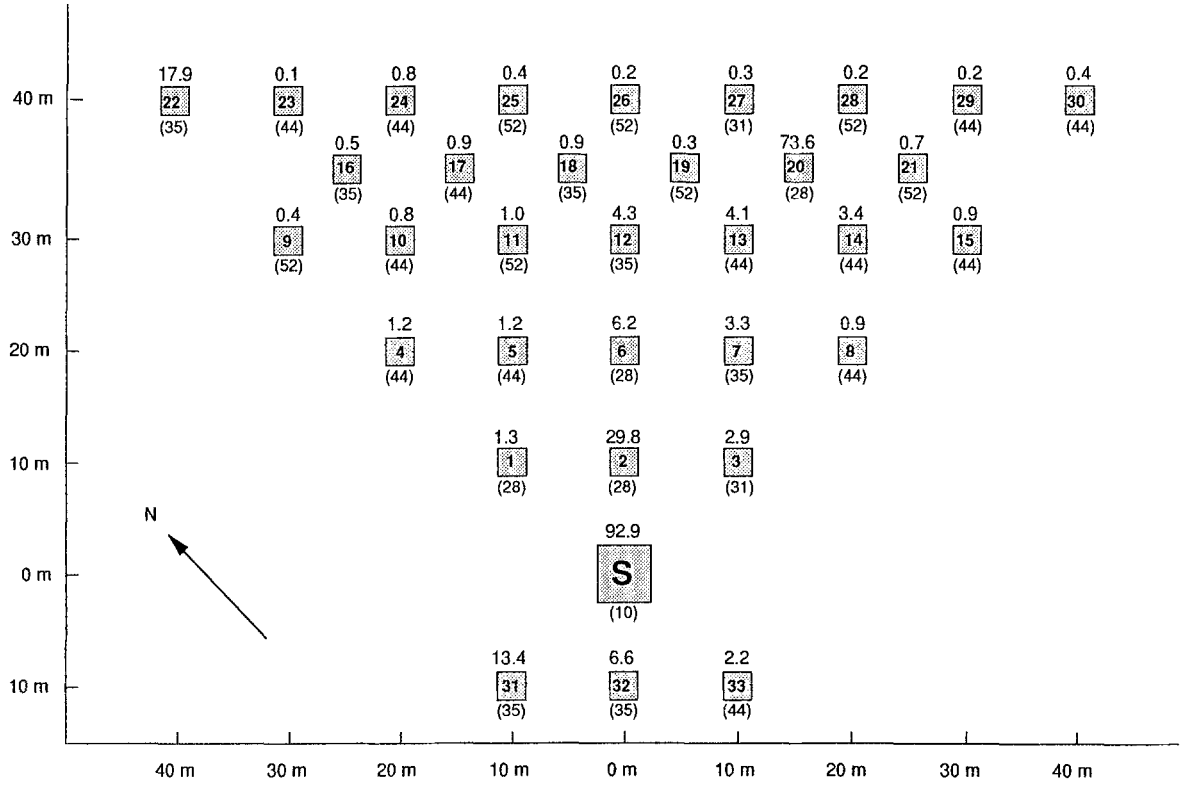

Fig. 1. Layout of the faba bean plots in a maize field. The vertical axis represents the direction of the prevailing wind (SW). Entries above plots are mean severity values per plot (%) at the end of the experiment (day 59). Entries below plots are times of first rust detection per plot. Source plot is labelled with bold S. Trap plots are labelled with bold numbers.

was negatively correlated with the distance from the source plot ($r = -0.60$, $P = 0.003$). In all cases, time of first rust observation and final disease severity were not correlated with the angle between plot location and prevailing wind direction ($P = 0.09$–0.50).

Representative disease progress curves for trap plots are shown in Fig. 4. All curves had an exponential pattern, indicating that epidemics in the trap plots began too late to reach saturation. The range of apparent infection rates in trap plots was $r_t = 0.19$–$0.38\ d^{-1}$. There was no correlation between the apparent infection rate of a trap plot and either its distance from the source plot ($P = 0.23$) or the angle between its location and prevailing wind direction ($P = 0.49$).

The individual epidemics from all trap plots were combined into a single trap-plots epidemic by averaging severity values per plot over distance to the source plot. The primary disease gradient of the trap-plots epidemic was induced by the spores emitted by the source plot during its infectious period and causing infections in the trap plots. The infectious period of the source plot extended as long as sporulating lesions were present in the source plot, i.e., from days 10 to 59, so the primary gradient was established at the end of the experiment, on day 59. Either the power law ($R^2 = 0.26$, $P = 0.04$, slope $B = 1.70$) or the exponential ($R^2 = 0.38$, $P = 0.006$, slope $B = 0.07\ m^{-1}$) models poorly described the disease gradient. When the two trap plots #20 and #22 were excluded, the disease gradient was much better described by both the power law ($R^2 = 0.64$, $P < 0.001$, slope $B = 2.11$) and the exponential ($R^2 = 0.65$, $P < 0.001$, slope $B = 0.08\ m^{-1}$) models.

Relationships between source-plot and trap-plots epidemics. The focal and classical models had similar coefficients of determination for the trap plots, but the focal model had a higher coefficient of determination for the source and for all plots combined (Table 1).

Goodness-of-fit of the focal model was further evaluated by plotting back-transformed estimates of severity values against observed severity values. The focal model correctly fitted the source plot (Fig. 5A)

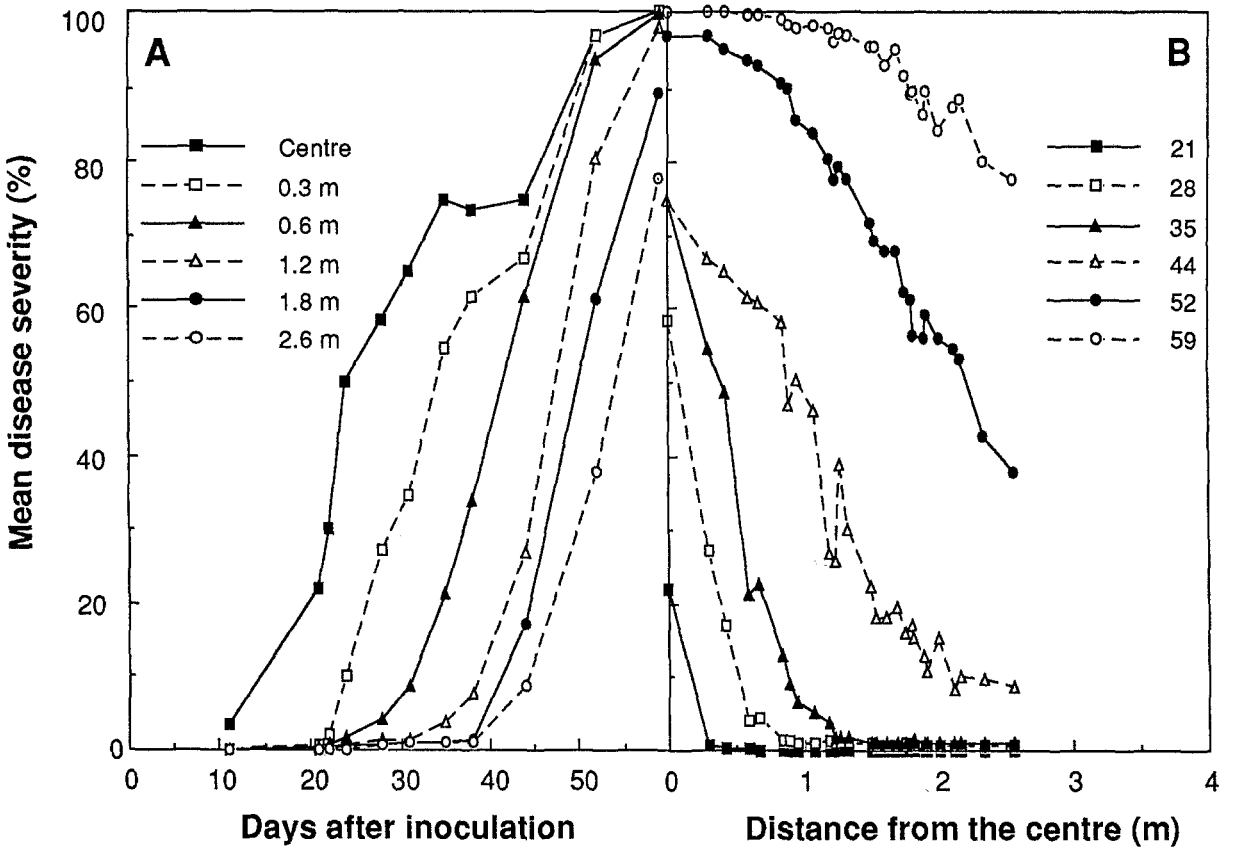

Fig. 2. Source plot. A. Disease progress curves for six selected distances from the centre. B. Disease gradients at six selected times (in days after inoculation).

Table 1. Parameter values obtained by multiple regression fitting logit $(x) = a_c - b_c.d + r_c.t$ (classical model) and logit $(x) = a_f - b_f.\ln(d) + r_f.t$ (focal model) to the mean disease severities (x) at various distances (d) from the inoculated unit and at various times (t) during the course of faba bean rust epidemics

Scale	Classical model					Focal model			
	R^2	b_c (m^{-1})	r_c (d^{-1})	SE[a]	α[b] (m)	R^2	b_f	r_f (d^{-1})	SE
Source plots	0.92	1.95 ± 0.09[c]	0.24 ± 0.01	0.84	0.5	0.95	2.00 ± 0.08	0.25 ± 0.01	0.67
Trap plots									
All	0.58	0.04 ± 0.02	0.27 ± 0.02	2.22	25.0	0.58	1.10 ± 0.51	0.27 ± 0.02	2.20
All but #20 and #22	0.87	0.11 ± 0.01	0.32 ± 0.01	1.16	9.1	0.86	2.78 ± 0.30	0.32 ± 0.01	1.21
Source and trap plots									
All	0.72	0.20 ± 0.01	0.23 ± 0.01	2.05	5.0	0.89	2.28 ± 0.06	0.25 ± 0.01	1.29
All but #20 and #22	0.81	0.24 ± 0.01	0.24 ± 0.01	1.71	4.2	0.95	2.54 ± 0.04	0.26 ± 0.01	0.92

[a] Standard error of estimate.
[b] Relaxation distance for disease severity, calculated as $\alpha = 1/b_c$ [Zadoks & Schein, 1979].
[c] Parameter estimate ± standard error.

and the trap plots, excluding the two plots #20 and #22 (Fig. 5B, closed circles). When the two plots #20 and #22 were included, the trap plots were poorly described by the focal model (Fig. 5B, open circles). When a single epidemic was assumed to occur over source and trap plots, the low disease severity observed in most

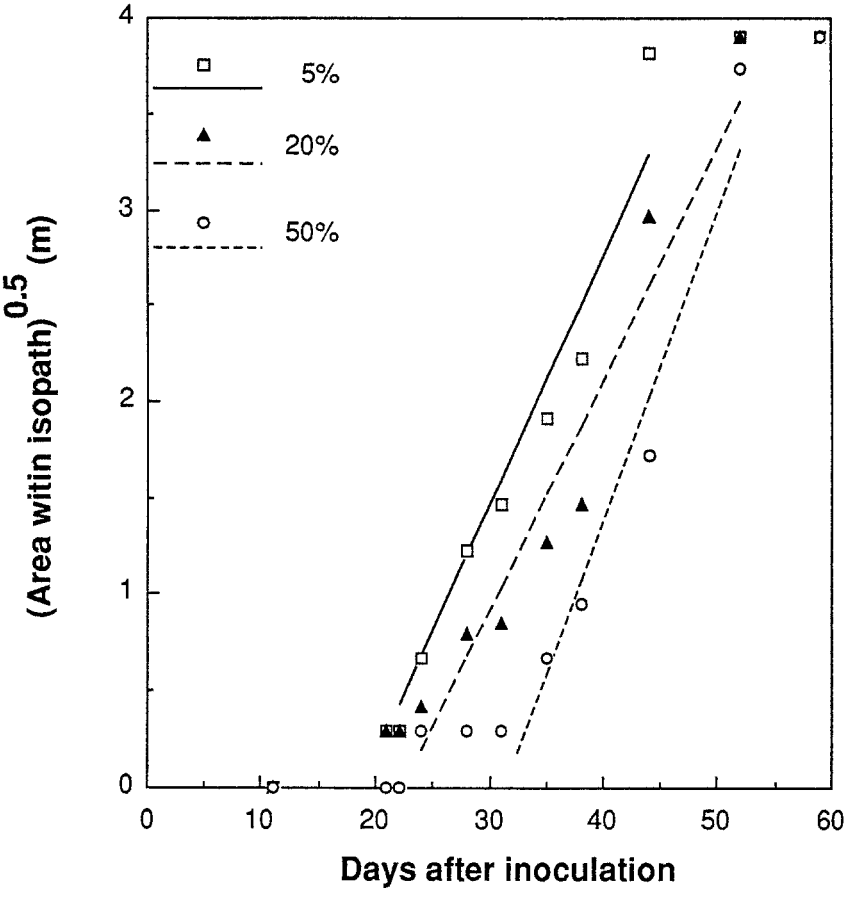

Fig. 3. Soure plot. Development of the square root of the area within an isopath with increasing time after inoculation for three isopath values. Regression lines were used to estimate the radial velocity of expansion.

trap plots was overestimated by the model, whether the two trap plots #20 and #22 were included (Fig. 5C) or excluded (Fig. 5D). The values of the time parameter (r_c and r_f) were only marginally influenced by the model and the scale of the epidemic (Table 1). For each model, the r value was smaller when the source plot was included than when it was excluded, and the highest r value was found in the trap plots, excluding the two plots #20 and #22. In the contrary, gradient parameters (b_c and b_f), which cannot be directly compared due to their different dimensions, considerably varied with the scale of study. The effect of the scale of study on the distance parameter was highlighted by considering the relaxation distance α. Upscaling the epidemics from the source plot to the whole field caused a tenfold increase in α. The effect of the two plots #20 and #22 on α was important only when epidemics occurring in the trap plot and over all the source plots were considered separately (Table 1).

Discussion

The source-plot epidemic. The epidemic occurring in the source plot followed a focal pattern, with no apparent directional effects. Turbulent diffusion of smoke puffs [Zadoks *et al.*, 1969] and rust spores may overcome dominant wind direction, when the wind is not too strong. The 'focal' model (equation [6]) fitted the epidemic in the source plot better than did the 'classical' (equation [5]) one (Table 1). The dominant mechanism, at least during the first weeks of epidemics, was a reinforcement of the primary gradient due to predominant autoinfection at the plant level. This autoinfection conserved the shape of the gradient (Fig. 2B) and increased the level of disease in a parallel manner across the plot (Fig. 2A). The same pattern of disease progress was observed in bean rust (caused by *Uromyces appendiculatus*) epidemics initiated by a linear inoculum source [Aylor

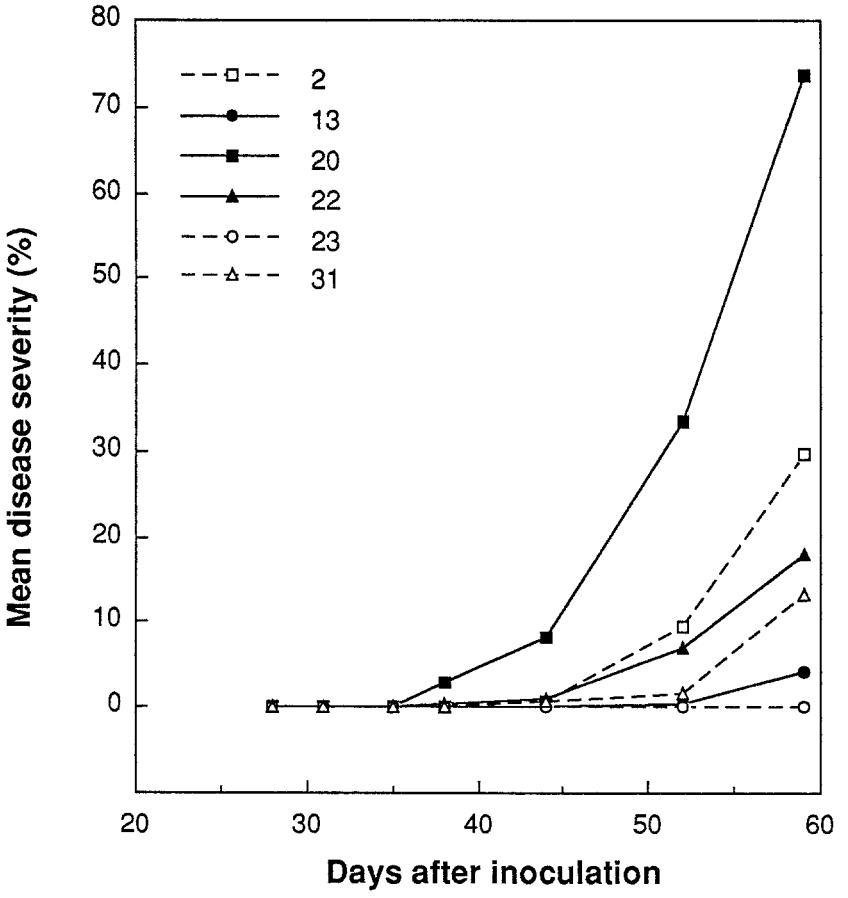

Fig. 4. Disease progress curves for six selected trap plots. See Fig. 1 for plot location.

and Ferrandino, 1989]. Using the 'focal' model, these authors found rate parameters in the same range (r_f = 0.19–0.31 m.d^{-1}) as ours, but shallower gradient parameters (b_f = 1.05–1.75). The difference may be explained by the geometry of the source [Gregory, 1968] and the length of the plot (30 m), and by differences in environmental conditions, varietal susceptibility, and canopy structure. The source-plot epidemic caused by the primary focus resulted in a travelling wave expanding with a constant radial velocity, as expected from theoretical considerations [Minogue and Fry, 1983a; Van den Bosch *et al.*, 1988b] and observed for various fungal, bacterial and viral plant diseases, as well as for insect infestations [Zadoks and Van den Bosch, 1994].

The trap-plots epidemic. Disease increased exponentially in each trap plot, as observed in the peripheral units of the source plot (compare Figs. 2A and 4). Final disease severity (Fig. 1), except for the plots #20 and #22 and some plots near the source plot, was comparable to disease levels recorded on naturally infected fields [Lapwood *et al.*, 1984]. In our discontinuous field, every trap plot, thus, can be considered as a secondary focus. However, great differences in final disease severity occurred between the trap plots and the unexpected high disease severity in the trap plots #20 and #22 is intriguing. Cross contamination between trap plots is unlikely to explain the high disease severity in plots #20 and #22, since the observer always entered the field by the upper-right corner and, thus, did not enter any heavily infected plot before reaching plots #20 and #22 (Fig. 1). Moreover, disease in the plots #20 and #22 was certainly induced by spores escaping from the source plot, because the contamination of the two plots #20 and #22 did not occur after the detection of sporulating lesions in the neighbouring trap plots (Fig. 1). The high severity in these two plots can be attributed to the landing of a heavy load of infec-

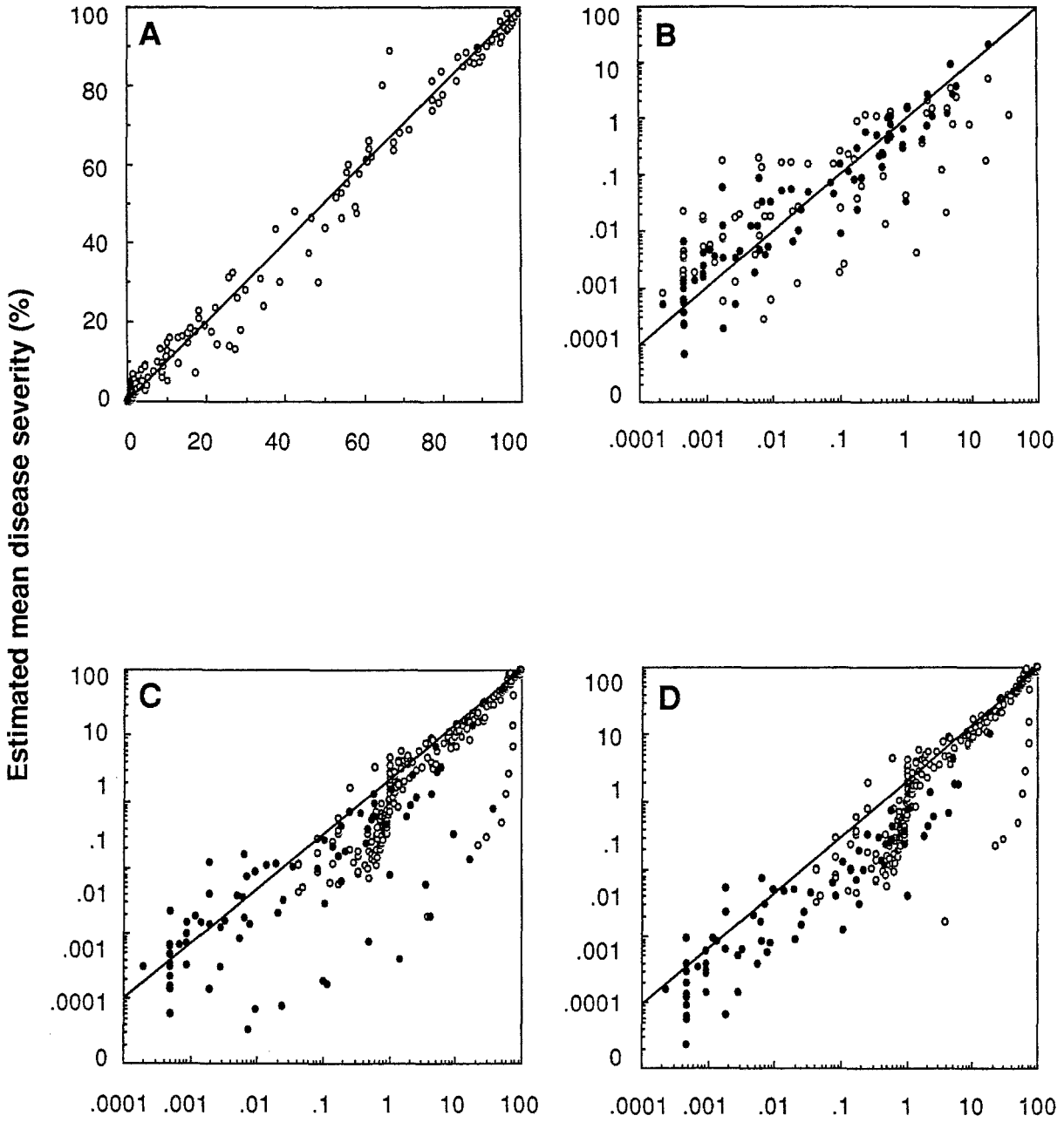

Fig. 5. Scatter plots of back-transformed estimated severity against actual severity. The model was $\text{logit}(x) = a_o + b_f.\ln(d) + r_f.t$, with x, mean severity, d, distance from the centre, and t, days after inoculation. Data were from A, source plot, B, trap plots including (open circles) or excluding (closed circles) the plots #20 and #22, C, source plot (open circles) and trap plots including the plots #20 and #22 (closed circles), D, source plot (open circles) and trap plots excluding the plots #20 and #22 (closed circles). Data were averaged over distances from target (unit for the source plot, plot for the trap plots) to inoculated centre.

tious spores, as well as to local environment highly favourable to disease development.

When individual epidemics occurring over each trap plot were combined into a 'trap-plots epidemic', the 'focal' and 'classical' models fitted equally well to the data (Table 1). High disease severity in the plots #20 and #22 strongly decreased goodness of fit of both models (Fig. 9B). When the two plots #20 and #22

were excluded, rate parameters (r_f and r_c) were not affected, but distance parameters (b_f and b_c) dramatically increased (Table 1). The trap-plots epidemic can not be considered as a travelling wave expanding with a constant radial velocity, and give a qualitative confirmation of the 'leaps and bounds' mechanism [Gäumann, 1946]. Secondary foci, considered as the result of a stochastic process [Zawolek, 1993] occurring at long distance and low frequency, might be explained by the dual dispersal mechanism postulated by Zawolek and Zadoks [1992].

The epidemic over the whole field. When the source-plot and trap-plots epidemics were combined into a single epidemic spreading over the whole discontinuous field, the model overpredicted disease severity at low disease levels in the trap plots, even when the two plots #20 and #22 were excluded (Fig. 5C–D). The combination of the two epidemics into a single one cannot correctly describe the spread of the epidemic at long distance from the source. We should rather consider a stratified process with a short-distance, deterministic dispersal in the source plot and a long-distance, stochastic, plot-to-plot dispersal over the discontinuous field. A similar stratification was described on larger scales for various examples of animal invasions by Hengeveld [1989], who stated that 'the establishments at large distances from the source location are often bridgeheads for further expansion far ahead of the wave front'. This statement qualitatively describes the appearance of disease in the trap plots, especially in the plots #20 and #22. Simulation models which combined neighbourhood diffusion and stochastic rare events of long-distance dispersal described, for example, the progress of foxes infected with rabies in central Europe [Hengeveld, 1989] and the invasion of flies in Australia [Mayer *et al.*, 1993]. Information about comparable mechanisms in plant disease epidemics is sparse. Classical studies of dispersal of urediniospores and aecidiospores of black rust of wheat (caused by *Puccinia graminis* f.sp. *tritici*) from point sources showed a focal pattern near the source associated with distant infections occurring on a 1–15 km scale [Johnson and Dickson, 1919; Stakman *et al.*, 1927; Schmitt *et al.*, 1959; Underwood *et al.*, 1959; Kingsolver *et al.*, 1984]. On a small scale, ergot disease of sorghum (caused by *Claviceps africana*) infected heads located at 15 m from the disease focus, well beyond the dispersal distance allowed by head-to-head contact and rainsplash [Frederickson *et al.*, 1993].

The dual-dispersal mechanism, thus, can be suggested to explain the observed pattern of disease progress in our experiment but was not definitively proved by our results. Firstly, we used a discontinuous field design for technical reasons. Fragmentation of plots and mixing with non-susceptible plants is known to reduce disease spread and intensification [e.g. Kiyosawa and Shiyomi, 1972; Zadoks and Kampmeijer, 1977; Lannou *et al.*, 1994]. It cannot be ascertained that the mixing effect was quantitative rather than qualitative, and that the experiment with a discontinuous field was representative of the same experiment made in a normal, continuous field. Secondly, it could be argued that distance parameter would increase with the spatial scale even if a single mechanism of spore dispersal is involved. Alternative models resulting in secondary focus formation with a single dispersal mechanism are available [Minogue, 1987; Shaw, 1994]. In these models, the epidemic spread is critically affected by the mathematical properties of the 'tail' of the function describing the primary disease gradient. In plant disease epidemiology, an extended gradient tail is usually attributed to background contamination from other spore sources [Gregory, 1968]. Gradient tails, however, may be longer than previously stated, as emphasized by Gäumann [1946] and demonstrated for seed dispersal gradients in higher plants [Portnoy and Willson, 1993]. Underestimation of the influence of the tail of the dispersal function might have induced underestimation of the radial velocity of expansion of various animal populations [Van den Bosch *et al.*, 1992]. More realistic models of disease progress should be based on a physical description of the mechanisms of spore dispersal leading to gradient formation [Ferrandino, 1993], but increasing model complexity will certainly decrease the attainable levels of abstraction and generality of epidemic theory.

References

Aylor DE and Ferrandino FJ (1989) Temporal and spatial development of bean rust epidemics initiated from an inoculated line source. Phytopathology 79: 146–151

Berger RD and Luke HH (1979) Spatial and temporal spread of oat crown rust. Phytopathology 69: 1199–1201

Ferrandino FJ (1993) Dispersive epidemic waves: I. Focus expansion within a linear planting. Phytopathology 83: 795–802

Frederickson DE, Mantle PG and De Milliano WAJ (1993) Windborne spread of ergot disease (*Claviceps africana*) in sorghum A-lines in Zimbabwe. Plant Pathol 42: 368–377

Gäumann E (1946) Pflanzliche Infektionslehre. Birkhäuser, Basel

Gregory PH (1968) Interpreting plant disease dispersal gradients. Annu Rev Phytopathol 6: 189–212

Hengeveld R (1989) Dynamics of Biologic Invasions. Chapmann and Hall, London

Jeger MJ (1983) Analysing epidemics in time and space. Plant Pathol 32: 5–11

Johnson AG and Dickson JG (1919) Stem rust of grains and the barberry in Wisconsin. Agric Exp Stn Univ Wisconsin, Bull 304: 1–16

Kingsolver CH, Peet CE and Underwood JF (1984) Measurement of the epidemiologic potential of wheat stem rust: St. Croix, U. S. Virgin Islands, 1954–57. Pa State Univ Agric Exp Stn Bull 854: 1–22

Kiyosawa S and Shiyomi M (1972) A theoretical evaluation of the effect of mixing resistant varieties with susceptible variety for controlling plant diseases. Ann Phytopathol Soc Japan 38: 41–51

Lannou C, De Vallavieille-Pope C, Biass C and Goyeau H (1994) The efficacy of mixtures of susceptible and resistant hosts to two wheat rusts of different lesion size: controlled condition experiments and computerised simulations. J Phytopathol 140: 227–237

Lapwood DH, Bainbridge A, McEwen J and Yeoman DP (1984) An effect of rust (*Uromyces viciae-fabae*) on the yield of spring-sown field beans *Vicia faba*) in the UK. Crop Prot 3: 193–198

Mayer DG, Atzeni MG and Butler DG (1993) Spatial dispersal of exotic pests – the importance of extreme values. Agric Syst 43: 133–144

Minogue KP (1987) Diffusion and spatial probability models for disease spread. In: MJ Jeger (ed) Spatial Components of Plant Disease Epidemics (pp. 127–143) Prentice Hall, Englewood Cliffs, NJ

Minogue KP and Fry WE (1983a) Models for the spread of disease: Model description. Phytopathology 73: 1168–1173

Minogue KP and Fry WE (1983b) Models for the spread of disease: Some experimental results. Phytopathology 73: 1173–1176

Portnoy S and Willson MF (1993) Seed dispersal curves: behaviour of the tail of the distribution. Evol Ecol 7: 25–44

Savary S (1987) The effect of age of the groundnut crop on the development of primary gradients of *Puccinia arachidis* foci. Neth J Plant Pathol 93: 15–24

Schmitt CG, Kingsolver CH and Underwood JF (1959) Epidemiology of stem rust of wheat: I. Wheat stem rust development from inoculation foci of different concentration and spatial arrangement. Plant Dis Rep 43: 601–606

Shaw MW (1994) Modeling stochastic processes in plant pathology. Annu Rev Phytopathol 32: 523–544

Stakman EC, Kempton FE and Hutton LD (1927) The common barberry and black stem rust. USDA Farm Bull 1544: 1–29

Underwood JF, Kingsolver CH, Peet CE and Bromfield KR (1959) Epidemiology of stem rust of wheat: III. Measurements of increase and spread. Plant Dis Rep 43: 1154–1159

Van den Bosch F, Frinking HD, Metz JAJ and Zadoks JC (1988a) Focus expansion in plant disease. III: Two experimental examples. Phytopathology 78: 919–925.

Van den Bosch F, Hengeveld R and Metz JAJ (1992) Analysing the velocity of animal range expansion. J Biogeogr 19: 135–150

Van den Bosch F, Verhaar MA, Buiel AAM, Hoogkamer W and Zadoks JC (1990) Focus expansion in plant disease. IV: Expansion rates in mixtures of resistant and susceptible hosts. Phytopathology 80: 598–602

Van den Bosch F, Zadoks JC and Metz JAJ (1988b) Focus expansion in plant disease. I: The constant rate of focus expansion. Phytopathology 78: 54–58

Vanderplank JE (1963) Plant Diseases, Epidemics and Control. Academic Press, New York

Vanderplank JE (1967) Spread of plant pathogens in space and time. In: Gregory PH and Monteith JL (eds) Airborne Microbes (pp. 227–246) Cambridge University Press, Cambridge

Zadoks JC and Kampmeijer P (1977) The role of crop populations and their deployment, illustrated by means of a simulator EPIMUL 76. Ann NY Acad Sci 287: 164–190

Zadoks JC, Klomp AO and Van Hoogstraten SD (1969) Smoke puffs as models for the study of spore dispersal in and above a cereal crop. Neth J Plant Pathol 75: 229–232

Zadoks JC and Schein RD (1979) Epidemiology and Plant Disease Management. Oxford University Press, New York

Zadoks JC and Van den Bosch F (1994) On the spread of plant disease: a thoery of foci. Annu Rev Phytopathol 32: 503–521

Zawolek MW (1993) Shaping a focus: wind and stochasticity. Neth J Plant Pathol 99(Suppl 3): 241–255

Zawolek MW and Zadoks JC (1992) Studies in focus development: An optimum for the dual dispersal of plant pathogens. Phytopathology 82: 1288–1297